

## A clumped-foliage canopy radiative transfer model for a Global Dynamic Terrestrial Ecosystem Model II: Comparison to measurements

Wenze Yang<sup>a,\*</sup>, Wenge Ni-Meister<sup>a</sup>, Nancy Y. Kiang<sup>b</sup>, Paul R. Moorcroft<sup>c</sup>, Alan H. Strahler<sup>d</sup>, Andrew Oliphant<sup>e</sup>

<sup>a</sup> Department of Geography, Hunter College of the City University of New York, 695 Park Ave., New York, NY 10065, United States

<sup>b</sup> NASA Goddard Institute for Space Studies, New York, NY, United States

<sup>c</sup> Department of Organismic & Evolutionary Biology, Harvard University, Cambridge, MA 02138, United States

<sup>d</sup> Department of Geography and Environment, Boston University, Boston, MA, United States

<sup>e</sup> Department of Geography and Human Environmental Studies, San Francisco State University, San Francisco, CA, United States

### ARTICLE INFO

#### Article history:

Received 25 June 2009

Received in revised form 23 February 2010

Accepted 23 February 2010

#### Keywords:

Canopy radiative transfer

Foliage clumping

Comparison to measurements

### ABSTRACT

In a previous paper, we developed an analytical clumped two-stream model (ACTS) of canopy radiative transfer from an analytical geometric-optical and radiative transfer (GORT) scheme (Ni-Meister et al., 2010). The ACTS model accounts for clumping of foliage and the influence of trunks in vegetation canopies for modeling of photosynthesis, radiative fluxes and surface albedo in dynamic global vegetation models (DGVMs), and particularly for the Ent Dynamic Global Terrestrial Ecosystem Model (DGTEM). This study evaluates the gap probability and transmittance estimates from the ACTS model by comparing the modeled results with ground-based data, as well as with the original full GORT model and a layered Beer's law scheme. The ground data used in this study include vertical profile measurements of incident photosynthetically active radiation (PAR) in (1) mixed deciduous forests in Morgan-Monroe State Forest, IN, USA, (2) coniferous forests in central Canada, (3) mixed deciduous forests in Harvard Forest, MA, and (4) ground lidar measurements of the canopy gap fraction in woodland in Australia.

The model comparisons with these measurements demonstrate that the ACTS model achieves better or similar performance compared to the full GORT and the layered Beer's law schemes with regard to agreements with field measurements and computational cost. The ACTS model has excellent accuracy and flexibility to model the canopy gap probability and transmittance for various forest scenarios. Also, it has advantages relative to the currently widely used two-stream scheme through better radiation estimation for photosynthesis by accounting for the impact of both vertical and horizontal structure heterogeneity of complex vegetation on radiative transfer. Currently the ACTS is being implemented in Ent and will be further tested for how it improves surface energy balance and carbon flux estimates.

© 2010 Elsevier B.V. All rights reserved.

### 1. Introduction

In Ni-Meister et al. (2010), we developed a simple but physically-based canopy radiative transfer scheme for photosynthesis, radiative fluxes and surface albedo estimates in dynamic global vegetation models (DGVMs), and particularly for the Ent Dynamic Global Terrestrial Ecosystem Model (DGTEM). Canopy radiative transfer in a DGVM must take into account changing vegetation structure, particularly foliage clumping, to provide vertical profiles of photosynthetically active radiation (PAR) for calculation of photosynthetic activity, transmittance of radiation to the ground for the soil heat balance and accurate timing of snowmelt, and canopy albedoes for the land surface energy balance for general

circulation models (GCMs). The accurate representation of these variables is then important for predicting ecological, climate, and carbon dynamics.

To briefly summarize, the canopy radiative transfer scheme developed in Ni-Meister et al. (2010) provides an analytical expression for foliage clumping, combined with a two-stream scheme and description of the vertical foliage profile, in order to calculate light transmission in both horizontally and vertically heterogeneous tree canopies. The expression for foliage clumping is analytically derived from the 3D geometric-optical radiative transfer (GORT) model of Ni et al. (1997), based on geometric optical (GO) theory proposed by Li and Strahler (1988). The foliage profile is estimated based on statistical characterization of tree geometry, foliage distribution, and tree density (Ni-Meister et al., 2001). The analytical solution has the added constraint that crowns do not overlap. Vegetation gap fraction/uncattered transmittance is calculated via Beer's law modified by the clumping factor, applied to the layered

\* Corresponding author.

E-mail address: [Wenze.Yang@hunter.cuny.edu](mailto:Wenze.Yang@hunter.cuny.edu) (W. Yang).

foliage profile. For conifer forests, the ACTS model also takes into account the effect of the needle-to-shoot clumping. In addition, the effect of trunks and branches is incorporated from a scheme from Ni-Meister et al. (2008). Thus, the canopy radiative transfer model takes into account the effect of leaves, trunks, and branches on light transmission, absorption and reflection for multilayered and multispecies vegetation canopies. We call this analytical GORT scheme the analytical clumped two-stream model (ACTS). The purpose of this paper is to evaluate the ACTS model by comparing the modeled PAR transmittance and canopy gap probability with: (1) the full 3D GORT model of Ni et al. (1997), (2) a layered Beer's law scheme (in which the vertical foliage profile is not constant and is calculated based on the scheme in Ni-Meister et al., 2001), and (3) field measurements of radiation transmission. Several test sites are used in the following ecosystem types: temperate broadleaf deciduous forest, evergreen needleleaf forest, deciduous needleleaf forest, and evergreen broadleaf forest. These vegetation types are chosen to distinguish differences in leaf type and crown shape that would have different impacts on canopy radiative transfer.

## 2. Model evaluation

To fully evaluate the ACTS model, we compared measurements to vertical profiles of incident PAR as calculated by three model schemes: (1) the clumped, ACTS scheme, (2) the full 3D GORT model, and (3) the layered Beer's law. We also test the trunk scheme by comparing modeled PAR profiles with PAR measurements during the leaf-off season in winter. We selected multiple examples of four different plant functional types (see Table 1 for the locations of each site) and compared the modeled gap probability/transmittance with (1) ground tower based PAR profile measurements in mixed deciduous forest in Morgan-Monroe State Forest, USA, (2) ground mast based PAR profile measurements in conifer forests in central Canada, (3) balloon-based PAR measurements in mixed deciduous forests in Harvard Forest, MA, and (4) vegetation gap probability profiles measured by a full digitized hemispherical-scanning ground lidar (Echidna®) (Jupp et al., 2009; Strahler et al., 2008) in pine plantation and *Eucalyptus* forest in Australia. These data sets are independent, providing us more confidence in the model performance. The following sections describe the site description, field measurement and model parameterization for each site.

### 2.1. Morgan-Monroe State Forests (MMSF), IN

#### 2.1.1. Site description

One of our two broadleaf deciduous forest sites was at Morgan-Monroe State Forest (MMSF), an AmeriFlux tower site located at 39°19'N, 86°25'W in south-central Indiana, USA (Schmid et al., 2000). MMSF is a western deciduous broadleaf forest within the maple-beech to oak-hickory transition zone of the Eastern deciduous forest, with a mean canopy height near the tower of 27 m and a total area of 95.3 km<sup>2</sup>. Twenty-nine tree species have been identified in the area surrounding the tower with five tree species comprising 73% of the total basal area of 26 m<sup>2</sup> ha<sup>-1</sup>, and the average age of trees in the vicinity of the tower is approximately 55 years (Ehman et al., 2002; Oliphant et al., 2004, 2006).

#### 2.1.2. PAR measurements

Oliphant et al. (2006) measured incident PAR at this site from a narrow guyed tower, 30 m high, which protrudes through the canopy without disturbing the canopy structure. The tower was mounted with nine levels of PAR quantum sensors, including both point sensors (LI190SB, LiCor, Lincoln, NE) and line averaging sensors (LI191, LiCor, Lincoln, NE), and a BF3 sensor (Delta-T, Cambridge, UK) to measure global incident and diffuse radiation above

the canopy mounted at the top of the tower. The data used in this study contain continuous observations of PAR from 2003 to 2007 at a frequency of one measurement per 15 min.

PAR transmittance measurements were first normalized by the above-canopy observations, then averaged into multi-year monthly profiles, as shown in Fig. 1a. Within the 20 m × 20 m plot around the tower where we collected our tree geometry inputs, the maximum height is less than 27 m and there are taller trees outside of this area and also higher topography which may cast shadows to this area. In order to eliminate the systematic error, we rescaled the transmittance profile to set the value at 27 m as having a transmittance of 1 (for top of the canopy), and shown in Fig. 1b.

These profiles can be clearly divided into two groups: (1) measurements from May to October during the leaf-on season, and (2) measurements during the leaf-off season for other months. In order to decrease the variance, the leaf-on season is selected from June to September, and leaf-off season from November to February. The profiles for the leaf-on and leaf-off seasons show distinct features, so the averaged PAR transmittance profiles are averaged in these two periods for comparison. The canopy can be regarded as two-storied according to the transmission profile and detailed tree geometry data.

Based on incoming PAR measurements at the top of canopy on clear days, we developed an empirical formula to estimate the ratio of direct versus diffuse radiation,  $\rho_r$ , as a function of solar zenith angle ( $\mu_i = \cos \theta$ ,  $\theta$  is the solar zenith angle) using curve fitting to second order polynomials. For the leaf-on season with  $\theta$  ranges from 16° to 90°, we obtained:

$$\rho_r(\mu_i) = -0.84\mu_i^2 + 1.5\mu_i + 0.18 \quad (1)$$

For the leaf-off season with  $\theta$  ranges from 30° to 90°, we obtained:

$$\rho_r(\mu_i) = -1.3\mu_i^2 + 1.8\mu_i + 0.13 \quad (2)$$

These fits provide  $R^2 = 0.897$  for Eq. (1) and 0.856 for Eq. (2). Fig. 2 shows the fitting results.

#### 2.1.3. Model parameterization

The model vegetation input parameters were obtained from tree geometry measurements in a 20 m × 20 m grid around the guyed tower. The grid contained 85 trees, and the detailed geometry parameters available for each tree included the *xy*-coordinates, height, diameter at breast height (DBH), crown diameter and depth. Plant area index (PAI) was sampled in the middle of the growing season at each 2 m × 2 m grid point within the plot at 2 m above ground level using a pair of LiCor LAI-2000 sensors (LiCor Inc. Lincoln, NE) as described in Oliphant et al. (2006). As the measured PAI is actually a mixture of leaf area index, branch area index, and trunk area index, the measurement is of effective, clumped plant area and not actual plant area due to the nature of LiCor LAI-2000 measurement. To avoid double counting of clumping in the model, we first calculated the clumping factor to estimate unclumped actual area from the measurements, and then removed the trunk area index. The resultant LAI is recorded in Table 2. Trunk area index was estimated as half of the leaf-off PAI measurement. No data were available for actual trunk versus branch area, so we estimated their ratio from examining the trunk area from geometric calculations and comparing to the remaining leaf-off PAI. The half-half ratio is reasonable given pipe model theory, also.

The canopy can be regarded as a two-story canopy, according to the recorded tree height data and the measured canopy transmittance profile. In parameterization of the lower bound of the over-story canopy center,  $h_1$ , two approaches are tested to estimate the value given limited sampling. In the first approach, a window

**Table 1**  
General information of validation sites.

Site	Subsite	Latitude	Longitude	Species	PFT <sup>a</sup>	Reference or PI
MMSF		39.323	-86.413	Western deciduous broadleaf	DBF	Oliphant et al. (2004, 2006), Ehman et al. (2002)
BOREAS	SOJP	53.916	-104.690	Old jack pine	ENF	Sellers et al. (1997)
	SOBS	53.987	-105.117	Old black spruce	ENF	
Harvard	C2	42.537	-72.173	Oak and beech	DBF	Wofsy et al. (1993); Audrey Plotkin, personal communication
	C5	42.549	-72.176	Birch, maple and beech	DBF	
	D4	42.536	-72.175	Mixed deciduous	DBF	
	E5	42.538	-72.177	Hemlock	DNF	
Tumbarumba	Pine	-35.601	148.108	Pine plantation	ENF	Jupp and Lovell (2004), Jupp et al. (2005)
	Tower	-35.601	148.108	Eucalypt forest	EBF	

<sup>a</sup>PFT: DBF—deciduous broadleaf forest, ENF—evergreen needleleaf forest, DNF—deciduous needleleaf forest, EBF—evergreen broadleaf forest.

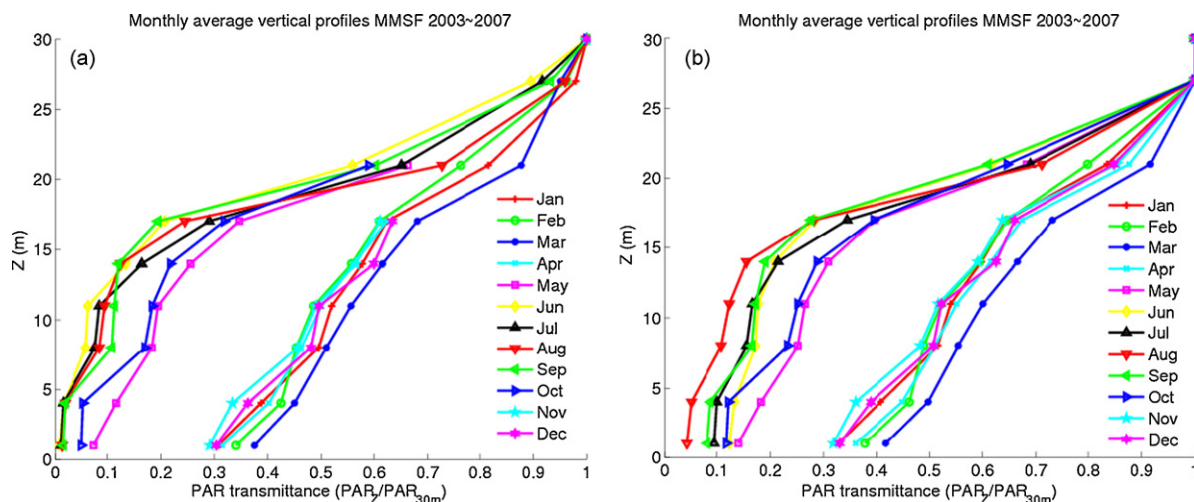


**Fig. 1.** Measured vertical PAR transmission profiles, averaged monthly through 2003–2007 in Morgan-Monroe State Forests (MMSF), IN, similar to Oliphant et al. (2006). (a) The reading at 27 m is not the same as 30 m due to topography or other impacts. (b) By setting 27 m as the canopy height, the transmittance profiles have been rearranged.

with fixed size is applied to the test site; all over-story trees falling into this window are used for the calculation of the crown center lower boundary height,  $h_1$ , by moving this window randomly within the site, a series of  $h_1$  is generated. In the second approach, a number of trees are randomly selected from the over-story canopy to calculate  $h_1$ , and a series of  $h_1$  is generated by repeating the random selection several times. One statistical result of the first approach is  $h_1 = 13.90 \pm 2.47$  m, and the second approach generates  $h_1 = 12.90 \pm 2.33$  m. Their overlapped region is the most probable value range of the over-story  $h_1$ .

## 2.2. Boreal forests, central Canada

### 2.2.1. Site description

For one of our two needleleaf forest sites, we used data from the Boreal Ecosystem–Atmosphere Study (BOREAS, Sellers et al., 1997), which was a large field campaign in central Canada conducted during the period of 1994–1997 in boreal forest in Canada.

The study site includes an old black spruce forest (*Picea mariana*) (SOBS) and an old jack pine forest (*Pinus banksiana*) (SOJP) in the Southern Study Area of BOREAS near Prince Albert and Candle

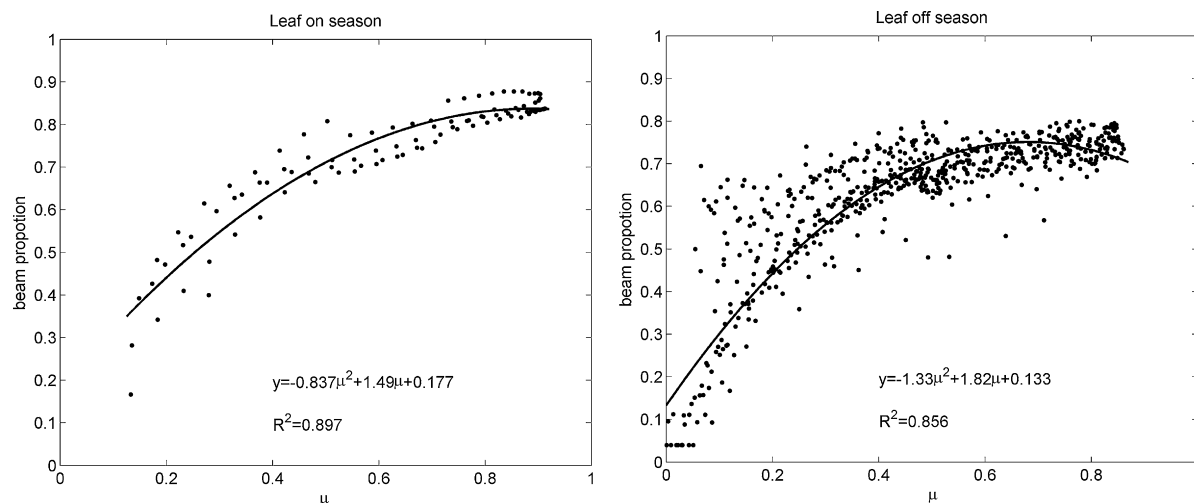


**Fig. 2.** Measured incoming direct beam portion and the fitted model for leaf-on and leaf-off seasons in 2003–2007 in Morgan-Monroe State Forests (MMSF), IN.

**Table 2**  
Tree geometry of validation sites as input for GORT.

Site	Subsite	$R$ (m)	$b$ (m)	$\lambda$ ( $\text{m}^{-2}$ )	$P_a$ ( $\text{m}^2 \text{m}^{-3}$ )	$h_1$ (m)	$h_2$ (m)	DBH (m)	$b/R$	PAI
MMSF	Leaf-on – upper	3.17	3.39	0.068	0.343	13.81	23.82	0.223	1.07	3.30(a)
	Leaf-on – lower	2.00	1.27	0.145	0.455	4.18	5.55	0.087	0.63	1.40(a)
	Leaf-off – upper	3.17	3.39	0.068	0.038	13.81	23.82	0.223	1.07	0.36(a)
	Leaf-off – lower	2.00	1.27	0.145	0.045	4.18	5.55	0.087	0.63	0.14(a)
BOREAS	SOJP	1.20	3.50	0.200	0.450	7.70	12.70		2.92	1.90(b)
	SOBS	0.76	2.65	0.405	0.874	3.03	8.51		3.49	2.27(b)
Harvard	C2 – upper	3.22	4.85	0.045	0.725	15.67	16.74		1.51	6.81(c)
Forest	C2 – lower	0.39	1.51	0.121	3.019	3.29	4.97		3.84	.36(c)
	C5 – upper	2.08	3.58	0.051	1.934	8.97	15.49		1.72	6.4(c)
	C5 – lower	0.44	1.54	0.232	5.380	3.46	7.18		3.45	1.59(c)
	D4 – upper	3.05	5.24	0.060	0.532	14.61	15.91		1.72	6.55(c)
	D4 – lower	0.51	1.37	0.191	5.292	3.87	5.65		2.67	1.51(c)
	E5 – upper	2.50	4.86	0.099	0.551	12.35	12.97		1.94	6.93(c)
	E5 – lower	0.48	2.45	0.070	2.559	3.43	3.85		5.11	0.42(c)
Tumbarumba	Pine	5.70	8.04	0.012	0.152	23.15	29.00	0.530	1.41	1.99(d)
	Tower – upper	3.33	6.78	0.013	0.350	25.66	36.89	0.694	2.04	1.43(e)
	Tower – lower	0.97	1.57	0.066	2.200	6.99	17.91	0.146	1.61	0.90(e)

a: Actual leaf and stem area index from LAI-2000 measurements (corrected for clumping and removed trunk).

b: Actual l shoot and branch area index measurements from Chen (1996) (first version of TRAC).

c: Actual plant area index from TRAC measurements.

d: Actual shoot area index with original needle area index calculated from allometric equations, corrected with shoot-level clumping.

e: Effective leaf and stem area index from hemispherical measurements.

Lake, Saskatchewan, Canada. The SOJP and SOBS sites are located at (53.916N, –104.690W) and (53.987N, –105.117W), respectively. The old black spruce forest stand is about 155 years old, 11 m tall trees with quite dense trees (about 5800 stems/ha). The old jack pine forest was about 75 years old, 15 m tall trees and relatively sparse (about 4000 stems/ha) compared to the old black spruce forest (Chen, 1996).

### 2.2.2. PAR measurements

During the 1994 summer field campaign, photosynthetically active radiation (PAR) measurements were collected on masts located in the SOBS and SOJP sites (Ni et al., 1997). Each mast in each site was equipped with a series of horizontal perches (or bars) at 2 m, 4 m, 6 m, 8 m and 10 m heights. Each perch had six equidistant optical sensors 0.3 m apart. The perches were southern-oriented with a small angle between them to avoid mutual shadowing. The measurements were collected every 10 min from sunrise to sunset almost every day during the BOREAS summer campaign. Averaged values of the PAR measurements from the six sensors at each level were used in this study. Because of differences in stem count density on the eastern and western sides of the mast in the SOBS site, we have only predicted PAR transmittance in the afternoon based on the stem count density on the western side of the mast.

### 2.2.3. Model parameterization

The tree geometry inputs for the two sites were from Chen (1996) and are shown in Table 2. The trees are quite uniform in the SOJP site, with a height range from 12 m to 15 m (Chen, 1996), while the tree heights and sizes at the SOBS site are non-uniformly distributed, with heights from 0 m to 11 m, with more tree height variation in the upper part of the canopy (see Ni et al., 1997). Thus the input parameters  $h_1$  and  $h_2$  for the SOBS site were calculated as  $h_1 = \text{mean}(h_c) - \text{std}(h_c)$  and  $h_2 = \text{mean}(h_c) + 3\text{std}(h_c)$ , where  $h_c$  is the crown center height and mean ( $h_c$ ), and std ( $h_c$ ) are the mean and standard deviation of the crown center height (Ni et al., 1997). Our model assumes that tree crowns are vertically randomly distributed in space following a Poisson distribution, which is a sufficient assumption within a canopy story. Shoots are treated

as the basic elements for these two conifer sites. Shoot-level PAI was obtained from Chen (1996) with correction of needle-to-shoot clumping on needle PAI values (see Table 2).

In modeling transmittance, both direct beam input and diffuse light were considered. The ratio of direct versus diffuse radiation on clear days was modeled as a function of solar zenith angle, as  $\rho_r(\mu_i) = \mu_i/(\mu_i + 0.09)$ , where  $\mu_i = \cos(\theta_i)$ , as described in detail in Ni et al. (1997).

### 2.3. Harvard Forest, MA

#### 2.3.1. Site description

We collected original PAR data for several mixed broadleaf deciduous stands and one hemlock (deciduous needleleaf) stand at Harvard Forest, Massachusetts, a Long Term Ecology Research site established in 1989 in Petersham, MA. Harvard Forest (42°32'N, 72°11'W, elevation 340 m) is a 60–70 year old mixed deciduous forest. The stands are in the transitional hardwoods-white pine-hemlock zone and are comprised mainly of red oak (*Quercus rubra*), red maple (*Acer rubrum*), yellow birch (*Betula alleghaniensis*), white birch (*B. papyrifera*), beech (*Fagus grandifolia*), white pine (*Pinus strobes*), and hemlock (*Tsuga Canadensis*).

#### 2.3.2. PAR measurements

We conducted balloon-based PAR data in three mixed deciduous broadleaf plots and one hemlock-dominated ecological monitoring plot west of the Environmental Monitoring Station (EMS) tower, in the Prospect Hill tract of Harvard Forest during summer 2006. A helium balloon of diameter 0.9 m and height 3 m with a PAR sensor mounted at the top was released to the top of the canopy. This diameter was small enough to pass through branches and foliage gaps. Then the balloon was pulled down manually with the initial height above the top of the canopy, and the PAR measurements were recorded automatically five times at height level increments of 1 m as integrated transmittances for direct and diffuse beam radiation. In each plot, four sets of measurements in four directions around the plot center were made for spatial averaging. Most recordings were collected on sunny days, though the sky was not completely clear most of the time with thin cirrus clouds passing

over. To distinguish direct versus diffuse radiation, we used the canopy top measurement as direct plus diffuse radiation, and then in an open area, we shaded the sensor for reference measurements for diffuse radiation.

### 2.3.3. Model parameterization

Tree ground measurements include stem map data including diameter at breast height (DBH), species, and canopy position for each individual tree by Barford et al. (2001). We collected plant area index data using tracing radiation and architecture of canopies (TRAC) during summer 2008. Other model structure inputs were estimated from a stem map using allometric equations (Albani et al., 2006) (see Table 2). Two canopy layers distinguishing upper story and understory (the division determined by the shape of measured PAR profile) were modeled in these sites.

## 2.4. Woodlands, Tumbarumba, Australia

### 2.4.1. Site description

Two sites were used near a flux tower location in Southeastern New South Wales, Australia, representing two different plant functional types: a pine plantation (referred to as the “pine site”) for evergreen needleleaf, and a *Eucalyptus* forest near the flux tower site (referred to as the “tower site” in this study) for evergreen broadleaf forest. The pine site is a uniform plantation without extensive understory. The *Eucalyptus* forest is moderately open and has an average tree height of roughly 40 m. The canopy is roughly divided into two layers. There is also significant ground cover of shrubs and grasses (see Jupp et al., 2009; Strahler et al., 2008, for details.)

### 2.4.2. Ground lidar measurements

Below-canopy ground lidar measurements using the Echidna® Validation Instrument (EVI), developed by CSIRO Australia as part of its canopy lidar initiative, were acquired in the pine site and the Eucalypt forest in a square plot arranged around the Tumbarumba Flux Tower in November 2006 (Jupp et al., 2009; Strahler et al., 2008). EVI is a ground-based, upward hemispherical-scanning, full waveform digitized, terrestrial lidar instrument and allows acquisition of vegetation canopy gap probability and related structure parameters, including height, basal area, stem counts, foliage profile and above ground biomass (Jupp et al., 2009, 2005; Jupp and Lovell, 2004; Strahler et al., 2008; Ni-Meister et al., 2008, in press).

We processed the EVI data to generate gap probabilities at different zenith ring ranges based on the method described in Jupp et al. (2009). In this study, we compared the modeled and EVI-measured gap probabilities to evaluate the model performance.

To compare GORT model results with EVI-based gap probability, we found that ground lidar based gap probability has an opposite pattern from the one modeled with incident light from the canopy top, and there is a strong trunk effect on the gap probability (Ni-Meister et al., 2008). Ni-Meister et al. (2008) extended the full GORT model to include both the trunk and foliage effects on the canopy gap probability. Their study has already demonstrated that the trunk effect is essential in modeling the gap probability for the below-canopy lidar. Here we ran our analytical leaf-and-trunk model and compared the inverted gap probability (from bottom to top of the canopy instead of top to bottom) with the upward-pointing lidar results of EVI measurements.

### 2.4.3. Model parameterization

The same set of model input parameters as in Ni-Meister et al. (2008) was used (see Table 2). The required parameters were measured in the field or extracted from the literature. At the pine site, the location and DBH of each tree in a 50 m radius plot were recorded in November 2006 (Strahler et al., 2008). At the 8 tower

**Table 3**

Foliage clumping factor as calculated by the analytical clumped two-stream (ACTS) model for the validation sites.

Site	Subsite	Clumping factor by zenith angle		
		0°	30°	60°
MMSF	Leaf-on – upper	0.69	0.69	0.70
	Leaf-on – lower	0.73	0.71	0.66
	Leaf-off – upper	0.94	0.94	0.95
	Leaf-off – lower	0.97	0.96	0.96
BOREAS	SOJP	0.84	0.90	0.93
	SOBS	0.79	0.89	0.92
Harvard Forest	C2 – upper	0.48	0.52	0.58
	C2 – lower	0.67	0.82	0.88
	C5 – upper	0.33	0.38	0.46
	C5 – lower	0.48	0.66	0.76
	D4 – upper	0.59	0.64	0.70
	D4 – lower	0.44	0.57	0.68
	E5 – upper	0.63	0.69	0.76
	E5 – lower	0.66	0.85	0.90
Tumbarumba	Pine	0.69	0.71	0.75
	Tower – upper	0.67	0.74	0.80
	Tower – lower	0.51	0.56	0.62

sites, variable radius plots were collected at each point using a 2 m<sup>2</sup>/ha basal area factor (Strahler et al., 2008). The upper and lower crown center heights,  $h_1$  and  $h_2$ , were extracted from EVI measurements. Tree size and density were calculated as mean values of all measured trees for the pine site but were weighted by the basal area for the tower site. Plant volume density ( $P_v$ ) was calculated from PAI, tree size and density measurements. The PAI values were obtained from Leuning et al. (2005). For the pine site, needle area index was calculated from allometric equations (Law et al., 2001) and converted to shoot area index using the method described in Ni-Meister et al. (2010) and  $\gamma_E = 1.25$  (Law et al., 2001). For the PAI parameterization of tower site, we obtained probable values from Leuning et al. (2005). For the tower site, PAI was estimated from fisheye photos measurements (Leuning et al., 2005).

## 3. Comparison of measurements and model estimates

The foliage clumping factor as calculated by the ACTS model is shown for all sites in Table 3, which lists the clumping factor for solar zenith angles of 0°, 30° and 60°. The sites demonstrate a good variability in clumping, allowing us to compare the different models' performance and examine how important foliage clumping is to the light profiles in different canopies. All of the sites exhibit a degree of clumping, except for the BOREAS sites, which have clumping factors generally greater than 0.8 due to dense stem density. Clumping factors decrease with increasing solar zenith angles. Morgan-Monroe State Forest was the only site with profile measurements available during the dormant (leaf-off) season, allowing us to test the effect of trunks and branches on PAR profiles. Reduced vegetation area index during the leaf-off season leads to an increased clumping factor compared to the leaf-on season.

The modeled gap probability and transmittance was developed at a stand scale. Fully evaluating the model requires that measurements are collected over a stand scale. However many field measurements were made at a point location, such as the measurements made on a tower. To compensate the problem, point measurements such as those collected in Morgan-Monroe State Forest and in boreal forests (SOJP and SOBS sites) were averaged in time bands to increase spatial samplings and then were compared with the modeled results.

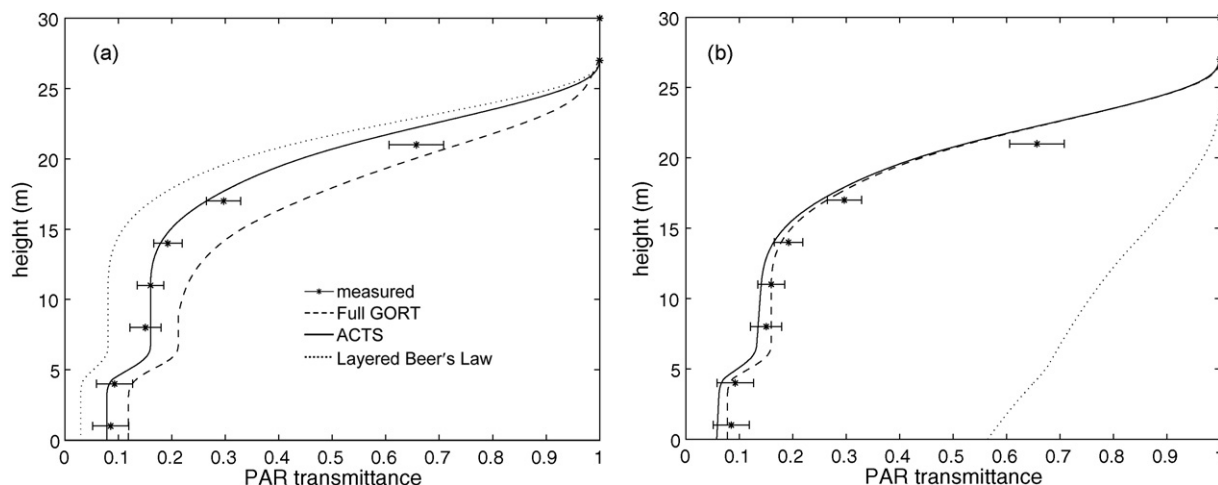


**Fig. 3.** Comparison of modeled and measured vertical distribution of PAR transmittance ( $T$ ) at the MMSF site for the leaf-on season. (a) Modeled results for the full GORT, ACTS and layered Beer's Law and (b) analytical clumped GORT model results when including leaf (dashed), trunk (dotted), and leaf + trunk (solid) in the model.

### 3.1. Morgan-Monroe State Forests, IN

The modeled and observed PAR profile comparison results of the leaf-on season are given in Fig. 3a. The observational monthly normalized averages are further averaged within the leaf-on season for each observed height level, and shown here are the mean and standard deviation at each height. The full GORT and ACTS modeling results fall within the observational range: the full GORT simulations fall at the high end, and the clumped analytical case falls nearly exactly at mean measured values at each height level. The layered Beer's law results fall slightly out of the observational range by underestimation.

Including the trunk effect in our model, in Fig. 3b, the transmittance at the bottom of the canopy decreases slightly relative to the model without the trunk effect, but the difference is within the error range of the measurements, implying that trunks have little effect on PAR transmittance in a full canopy of foliage.

In the winter when the trees are bare, there is negligible difference between the ACTS and layered Beer's law, as expected, as the forest is less clumped, while the full GORT overestimates transmittance due to assumption of more randomly rather than regularly spaced trees (Fig. 4b). The trunk effect in winter, in contrast to summer, has a major influence on PAR transmittance and is critical to include when there are few leaves on the trees. Fig. 4 demonstrates the significant difference between the model schemes with and without the trunk effect when there are no leaves, with exceptional fits to measurements with the trunk effect.

Note that the measured PAI value (using a LiCor-2000) is actually a vegetation area index. That is, the PAI value used in the model should be regarded as leaf area index + branch area index + trunks. We use the original PAI measurements in our model during leaf-on season and remove trunk area index from leaf-off PAI measurements in our simulation to avoid double counting the trunk effect. Trunk area index was estimated as half of total leaf-off PAI, following the rationale as explained earlier for Morgan-Monroe State Forest.

### 3.2. Boreal forests in central Canada

Modeled vertical PAR transmittance profiles and transmittance at the bottom of the canopy as a function of solar zenith angle were compared to the field measurements. Fig. 5 shows the comparison of the modeled vertical PAR transmittance using the ACTS, the full GORT and layered Beer's law with the PAR measurements in

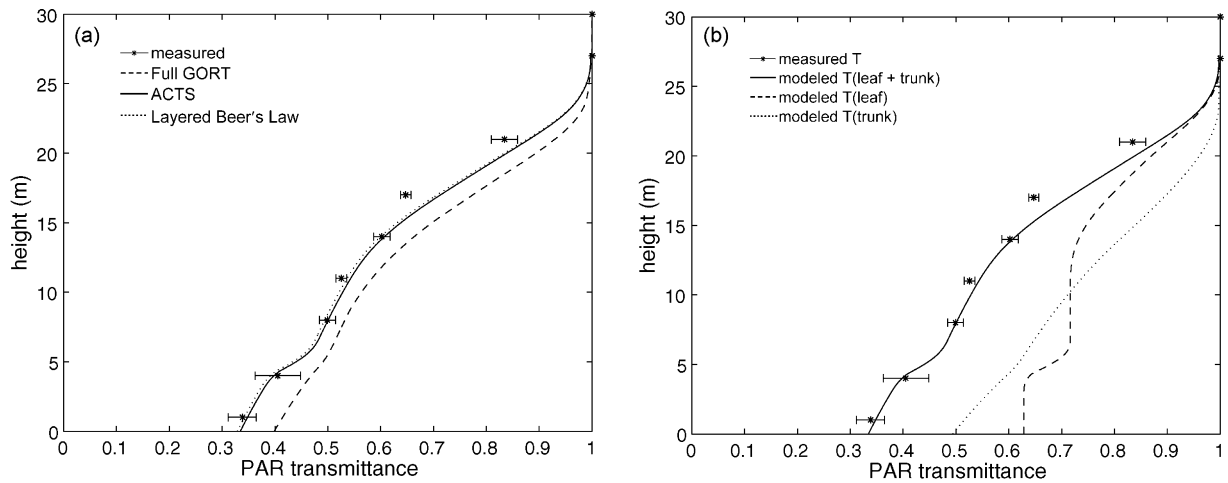
the SOBS and SOJP sites. These are averaged transmittance profiles of multiple solar zenith angles ranging from  $32^\circ$  to  $89^\circ$ . There is no significant difference among the three models' modeled PAR transmittances compared to the deviation in measurements. This is consistent with the stands being dense and therefore without a large clumping effect: the calculated clumping factors ranged 0.79–0.93 and in general  $>0.90$  at solar zenith angles greater than  $30^\circ$ . All modeled transmittance profiles show a sigmoid shape, with generally negligible deviation for the SOJP (Fig. 5a), and larger deviation from measurements at mid-canopy height for the SOBS site (Fig. 5b).

Fig. 5 shows a larger deviation of clumped ACTS from measurements in the SOBS site than in the SOJP site. One possible reason might be due to the non-uniformly distributed tree height and size in the SOBS site. The simple treatment to characterize the crown center height distribution as described in Section 2.2.3 might not be accurate enough. A more complicated approach might be necessary.

Fig. 6 shows the comparison of the modeled PAR transmittance by the three models and the ground measurements as a function of solar zenith angle (SZA). The three models capture the angular features shown in measured PAR transmittance, which looks like a hockey stick in that the transmittance decreases first as SZA increases, but at high SZA ( $>80^\circ$ ) the transmittance increases due to a large portion of radiation from the diffuse component. The mismatches between the modeled and measured transmittance at the small zenith angles ( $<55^\circ$ ) is due to the unrepresented saplings in the ground measurements (see Ni et al., 1997 for details).

Note that the predicted minimum in transmittance occurs at slightly larger solar zenith angles than the measurements indicate. One possible reason for this shift could be errors in the estimated proportions of beam and diffuse light. Despite the departure in the predicted minimum, the models provide a good enough approximation of the measured PAR transmittance at the bottom of forest canopies. Consistent with theory, the ACTS model estimates higher transmittance than the non-clumped layered Beer's law.

The models are very close in their results. However, Figs. 5 and 6 both show that the full GORT model shows even lower transmittance than the Beer's law model, whereas we would expect its allowance of overlapping crowns to tend toward overestimation of transmittance. We suspect that the full GORT model in this case departs from expected trends because of the high ellipticity of the trees, but this requires further investigation. Any model error is, at least, not significant, since predictions of all the models are quite



**Fig. 4.** Comparison of modeled and measured vertical distribution of PAR transmission at the MMSF site for the leaf-off (winter) season. (a) Full GORT, ACTS, and layered Beer's Law. (b) ACTS including leaf only, trunk only, and leaf + trunk.

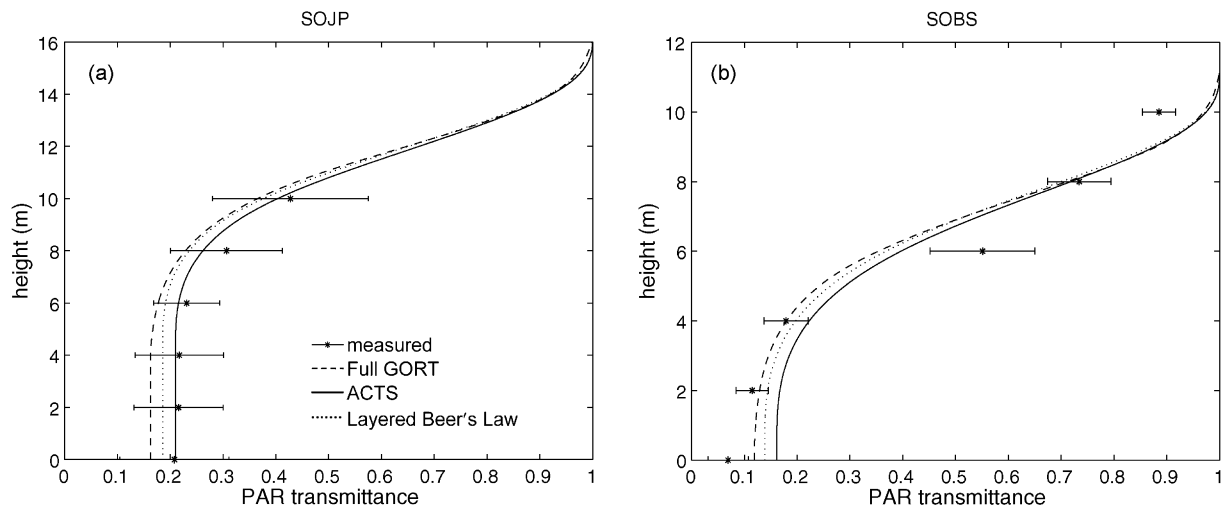


**Fig. 5.** Comparison of full GORT (dashed), ACTS (solid), layered Beer's Law (dot dashed) modeled and measured (error bar) vertical distribution of PAR transmission averaged between solar zenith angle from 32° to 89° in the BOREAS site for (a) SOJP stand and (b) SOBS stand of BOREAS in central Canada.

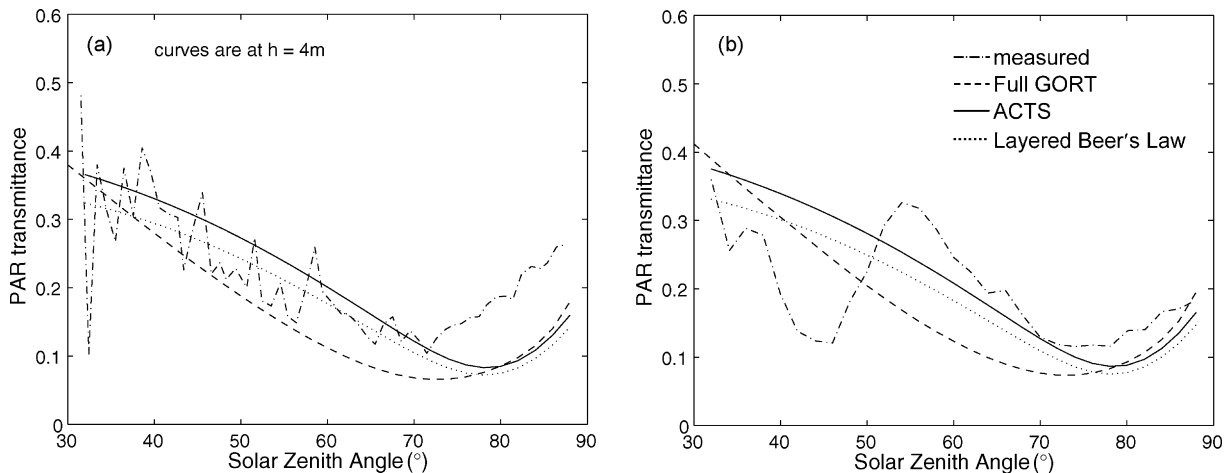


**Fig. 6.** Comparison of full GORT (dashed), ACTS (solid), layered Beer's Law (dotted) modeled and measured (dot dashed) PAR Transmission as a function of solar zenith angles in (a) SOJP stand and (b) SOBS stand of BOREAS in central Canada at a height of 4 m.

close, all within the range of measured variance, indicating that this stand overall has a fairly low level of clumping (clumping factor near 1).

### 3.3. Harvard forest, MA

Fig. 7 compares the modeled PAR transmittance profiles by the ACTS (red), the full GORT model (blue), and layered Beer's law (green) with the balloon data collected at four different plots and at different Sun positions (on different days); the mean observational data is shown in black, and the one standard deviation range is shown in the grey shaded area. In these validation sites, the solar zenith angle spanned from 20.2° to 71.8°, and the atmosphere conditions ranged from clear sky to thin cirrus clouds. In all cases the ACTS modeled PAR profiles fall between the layered Beer's law and the full GORT, as expected. The analytical clumped GORT will always be intermediate between the layered Beer's law and the full GORT. How close or different they are tells us about the properties of the canopy. At large solar zenith angles (>50°), the clumped analytical and the full GORT models have similar results.

Some deviation of all the model results from the measurements in the upper part of the canopy exists for the C2, C5, and E5 sites (Fig. 7a–c and f), where measurements show faster light extinction at the top of the canopy than the models, while at the canopy bottom there is lower (C2) or higher transmittance (C5, E5). This could be due to the nature of the balloon measurements, and the model parameters. The measured profiles are not smooth, since the balloon path sampled actual canopy gaps in a single vertical profile, rather than an average of several horizontally separated profiles. (It was not feasible to conduct a horizontal sampling of several vertical profiles given the constraints on measurement time.) As the balloon had to be pulled through a sufficient vertical opening in the canopy, the leaves of the topmost tree could occur on one side of the sensor so as either to immediately shade the sensor or to be completely out of the sensor view. This leads to the jaggedness of the measured profile. At the bottom of the canopy in C2, the tree demographic data was biased toward neglecting understory saplings below a certain DBH, whereas the balloon measurements capture these trees. In C5 and E5, greater measured transmittance at the bottom of the canopy could have been due to diffuse scattering by thin cirrus clouds that appeared during the understory measurements. Finally, the model parameterizations of the canopy geometry inputs were estimated based on allometric equations and are subject to error.

The modeling results all follow the balloon profile pattern in the same way regardless of the solar zenith angle at the measurement time, which spanned from 20.2° to 71.8°. At very high solar zenith angles (Fig. 7c), due to the very long path length, all models present a nearly zero transmittance at the bottom of canopy, while the measured values are much larger. The same issue happens to Fig. 7f. The reason for the underestimation could be the overestimated PAI value. More likely, intermittent cirrus clouds increased the fraction of diffuse radiation during the understory measurements compared to the canopy top and reference measurements, as mentioned earlier.

For other better measured cases, the overall comparison shows that the analytical and full GORT models predict better PAR profiles than the layered Beer's law even with vertical foliage variations. The ACTS model sometimes performs better than full GORT model by being closer to the balloon profile, and rectifying the overclumping assumption of the full GORT model in several cases.

### 3.4. Tumbarumba forest, Australia

Fig. 8 compares the pine site's averaged EVI-derived gap probability profiles within 20° bands of solar zenith angle range with

the modeled gap probabilities by the analytical leaf and branch and trunk and the full leaf-and-trunk GORT models and the layered Beer's law. The modeled gap probability represents canopy gap probabilities at the stand scale. With only one hemispherical EVI scan at the pine site, to make the model and observations inter-comparable, the EVI averaged gap probability in 20° zenith angle bands were compared (see Ni-Meister et al., 2008 for details on averaging). Fig. 8 shows very large standard deviations at small zenith angles. This indicates that EVI measurements are less representative for a stand scale at small zenith angles even if averaged within 20° bands. Note the discontinuous EVI gap probability profile of Fig. 8f is due to the averaging scheme: at height levels below 34 m, all four values are available; at height levels greater than 34 m, 65° values are not available, and at height levels greater than 39 m, 60° values are not available.

In general, both the analytical and the full GORT model results are consistently within the range of the standard deviation of EVI measurements. Even EVI data at small zenith angles containing some unrepresented sampling issue, the modeled gap probability profiles are still in the error range. The ACTS matches the best with the EVI measurements. Full GORT slightly overestimates EVI mean measurements. The layered Beer's law is outside the range at most zenith rings and underestimates EVI measurements, which means this canopy has significant foliage clumping, and validates the importance of implementing the clumping scheme in the ACTS model. The direct comparison between the ACTS and the full GORT suggests that the full GORT model might be too clumped, as the full GORT modeled gap probability slightly overestimates gap probabilities at small zenith angles in the upper part of canopy. At larger zenith angles, the clumped analytical clumped GORT and the full GORT have similar performance, reinforcing that foliage clumping must be a strong influence while the exact level of clumping is perhaps not precisely determined for this canopy. At the solar zenith angle range of 30–50° where the EVI measurements have the greatest precision, the ACTS model demonstrates a significantly better fit to measurements than the full GORT model. The modeled gap probability profiles in the lower part of canopy match very well with EVI-measured values, indicating the extended leaf-and-trunk GORT model is able to model the effect of woody structures on gap probabilities.

Fig. 9 shows the same comparison results as Fig. 8 but for the *Eucalyptus* site. Eight EVI scans were averaged to produce the averaged gap probability at different 5° zenith angle bands. The standard deviations of the eight EVI gap probability profiles show a similar decrease with zenith angle, also decrease with the zenith angle band width. A 5° zenith angle band width was therefore chosen for the *Eucalyptus* profiles. Fig. 9 shows very similar results in a two-layer forest canopy as shown in Fig. 8 in a single layer canopy. The ACTS model most consistently matches the EVI measurements at different zenith angle bands. Layered Beer's law underestimates the EVI measurements, while the full GORT results are still within the range of standard deviation of EVI measurements, indicating strong clumping in this canopy. Overall our comparison results between the modeled and EVI-measured canopy gap probabilities demonstrate that the ACTS modeled gap probability matches the best with the EVI measurements comparing with the results using the full GORT and layered Beer's law in one-layer or two-layer forest canopies.

### 3.5. Model vertical resolution sensitivity

Here we report the sensitivity of the ACTS model to vertical resolution using the geometry inputs in the MMSF site. In the ACTS theory development in Ni-Meister et al. (2010), we followed previous practice with the full GORT model, using a fine vertical resolution of 0.1 m to calculate radiation profiles. This resolution

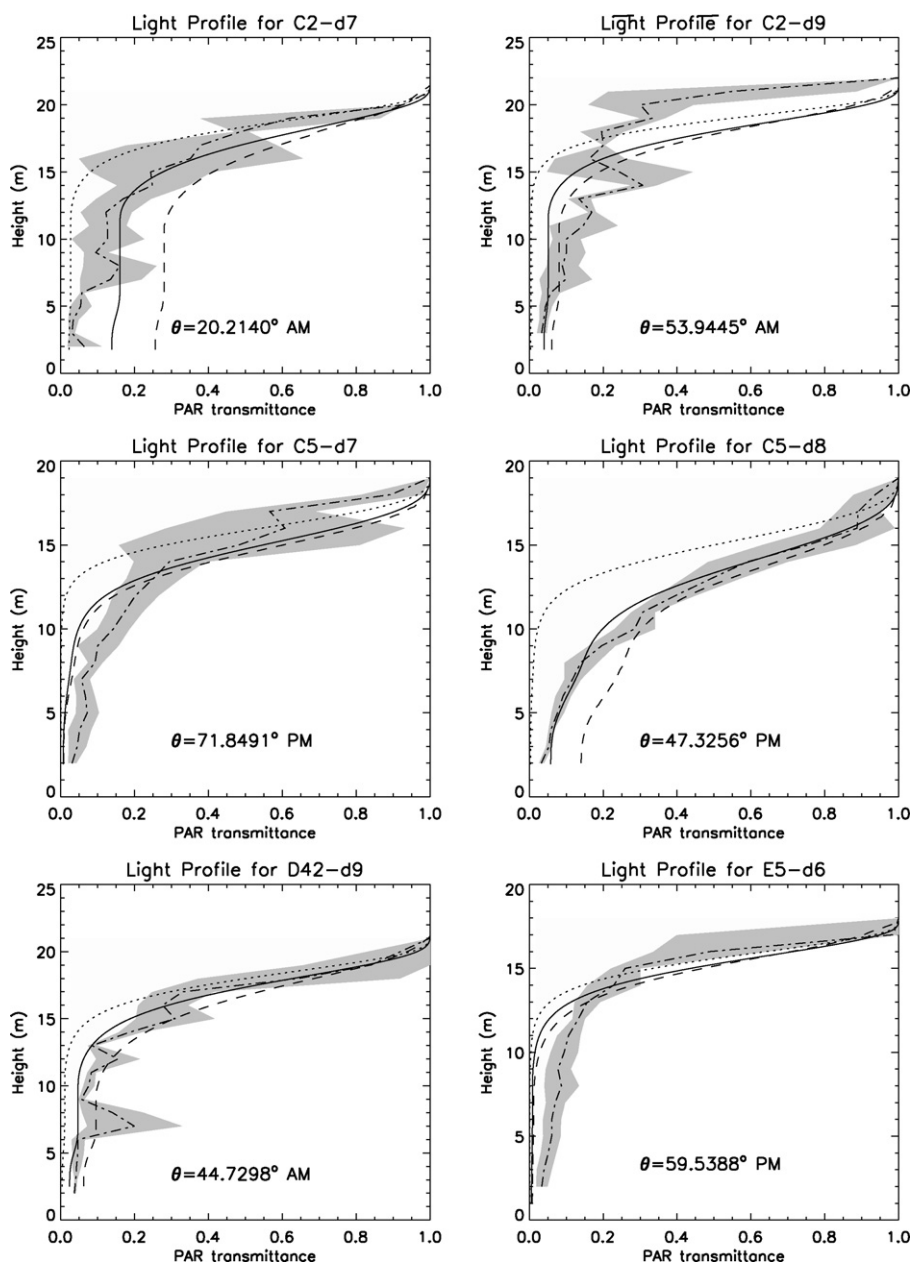


Fig. 7. Comparison of full GORT, ACTS clumped, ACTS, layered Beer's Law modeled and balloon measured vertical distribution of PAR transmission in Harvard Forest site for the following stands: (a) and (b) C2, (c) and (d) C5, (e) D4, and (f) E5.

may have a high computing cost for a dynamic vegetation model. Here we assess the vertical resolution that is minimally sufficient to retain a desired computational accuracy.

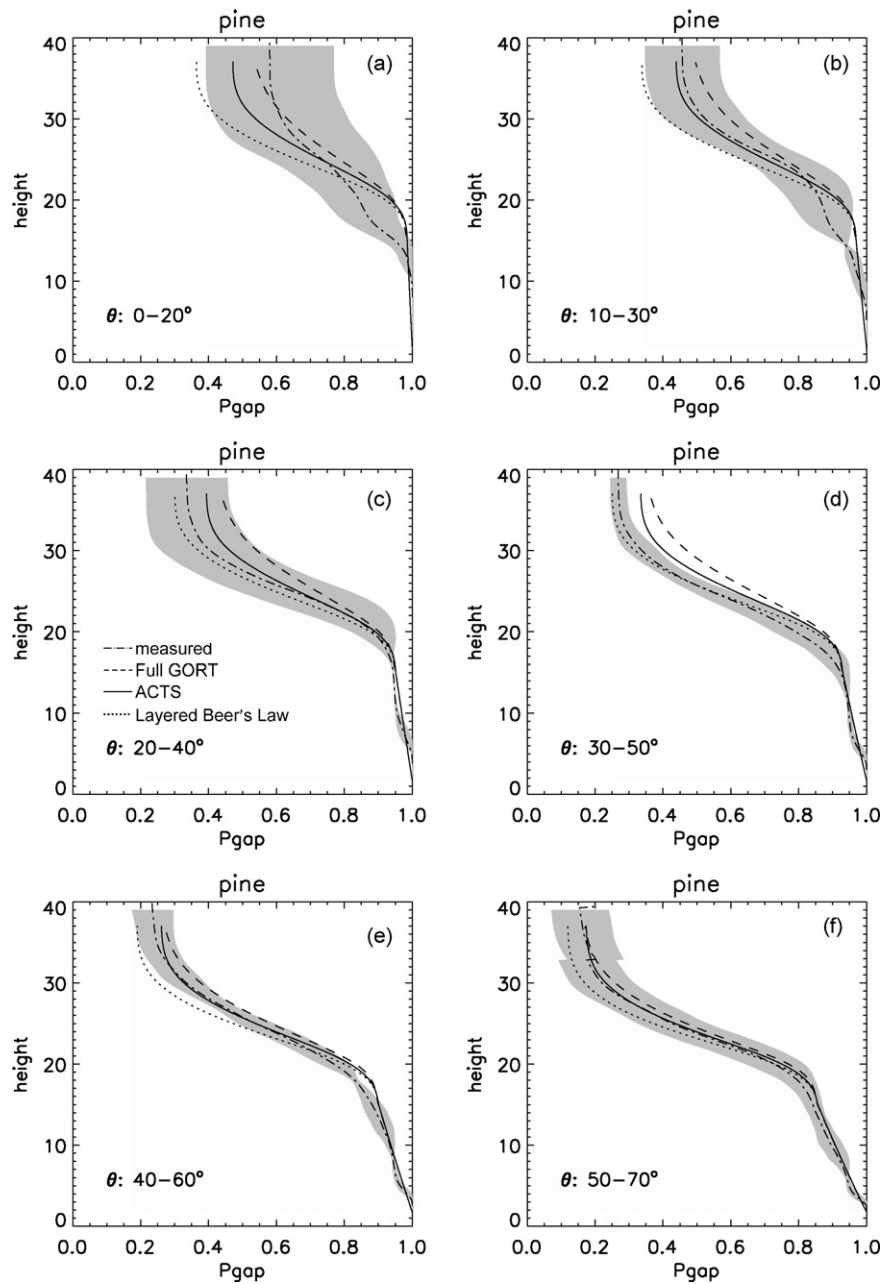
From the whole-canopy gap probability, we know the whole-canopy reflectance,  $R$ , and transmittance,  $T$ , and, given soil broad-band reflectance,  $\rho_s$  (we use 0.075 for 0.3–0.74  $\mu\text{m}$ , and 0.314  $\mu\text{m}$  for 0.74–1.35  $\mu\text{m}$  from Ni-Meister et al., 2010), we can calculate the whole-canopy absorbance,  $A$ , from the relation  $A + R + (1 - \rho_s)T = 1$ . To assess the impact of vertical resolution, we sum up the absorbance in layers,  $A_i$ , at varying resolutions and compare the difference between  $A$  and the sum of the  $A_i$ .

Table 4 provides the values for  $A$  and for the summed  $A_i$ , where the layering schemes range from 0.05 m to 10 m uniform layers. The calculation shows that at coarser resolutions, the total canopy absorption decreases, which holds true for both the visual band and near infrared band, and for both the ACTS and layered Beer's

law schemes. At the resolution of 0.1 m, the relative error is less than 0.2%. At the resolution of 10 m, this relative error increases to 21.8% for ACTS. A resolution of 2 m results in a relative error less than 4.9%, which might be an acceptable error for a DGVM or land surface model.

Table 4  
Sensitivity test of vertical resolution of the models, in term of absorbance.

Dz (m)	ACTS		Layered Beer's law	
	Abs_VIS	Abs_NIR	Abs_VIS	Abs_NIR
Ref	0.731	0.622	0.841	0.726
0.05	0.730	0.621	0.840	0.725
0.1	0.729	0.621	0.838	0.724
1	0.713	0.612	0.812	0.708
2	0.695	0.601	0.784	0.691
5	0.641	0.568	0.706	0.639
10	0.572	0.522	0.612	0.576



**Fig. 8.** Comparison of leaf+trunk full GORT, ACTS, layered Beer's Law and EVI-derived canopy gap probabilities ( $P_{\text{gap}}$ ) in  $20^\circ$  zenith angle bands in a pine plantation, Tumbarumba, New South Wales, Australia.

A dynamic vegetation model will not describe canopies with the same detailed level of variability as a natural canopy, so the higher resolution for canopy radiative transfer may not be necessary, except for possibly the top of the canopy, where the most light extinction occurs. GORT can be used to compute the radiation regimes at finer resolutions in the upper canopy, with height levels in the lower canopy at decreasing resolution or linked to explicitly tree layers as described by the dynamic vegetation model. Evaluation of the trade-offs between computational costs and model performance must be done through coupled simulations with a DGVM and land surface model.

#### 4. Discussion

Data limitations are the primary source of uncertainty in evaluating our model. Those factors include (1) measurement errors

e.g., the balloon measurements, allometric relations, (2) limited spatial samplings, e.g., the tower/mask (MMSF, SOJP and SOBS) measurements and (3) accurate model parameterization. Balloon inaccuracies were previously mentioned, so here we mainly discuss the other two factors.

In all of the site measurements where only a single point location for a vertical profile could be measured (i.e., no areal averaging could be done), the true canopy mean of the vertical light and foliage profiles cannot be known from the sample, particularly at the very top of the canopy. However, varying solar zenith angles helps to provide an average profile lower down in the canopy, and we still are able to demonstrate where clumping is a significant factor for modeled profiles.

As with all other models, correct parameterization for the ACTS model is critical and also challenging. Measurements for validation are also subject to error. In our validation sites, the scale of measure-

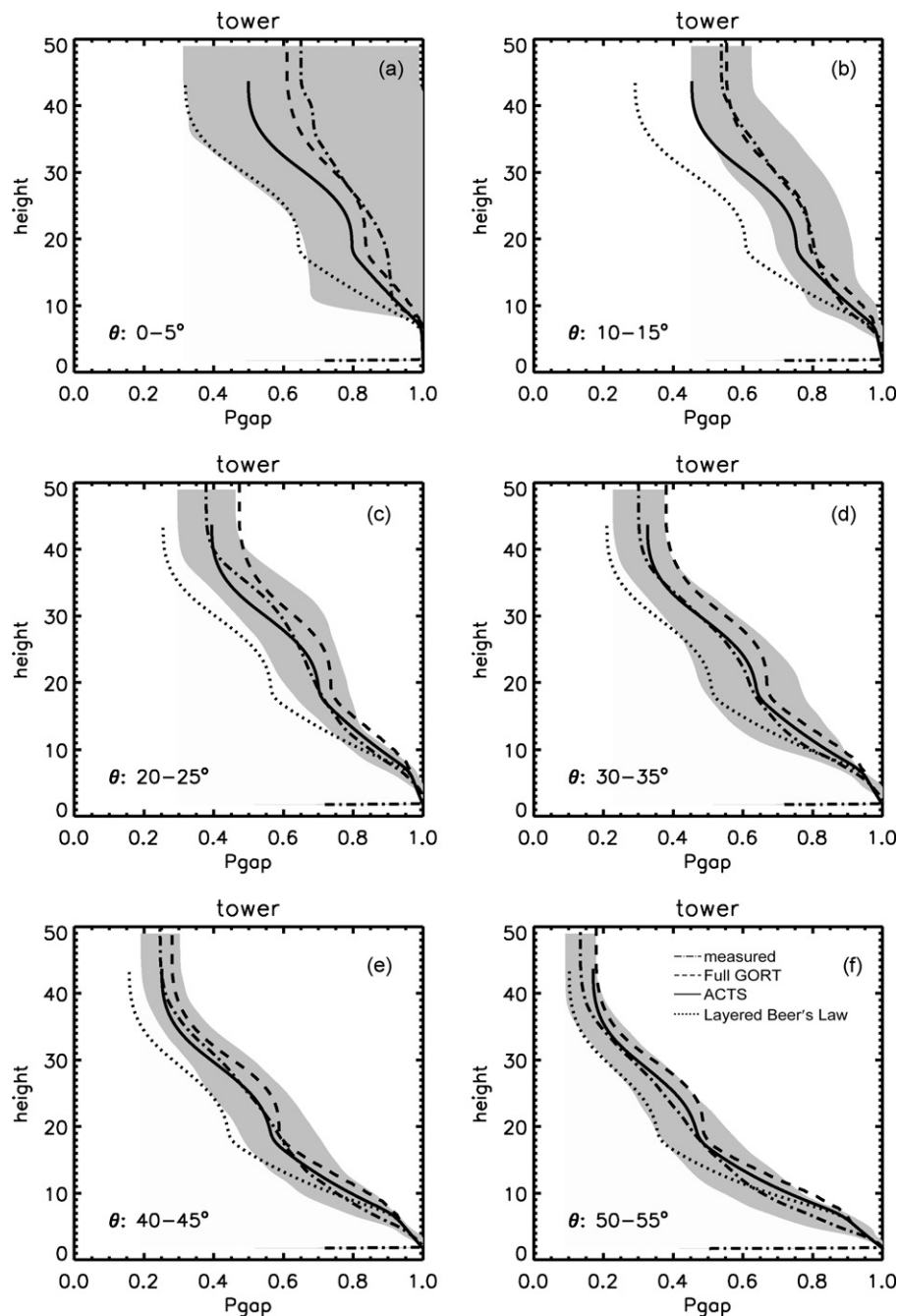


**Fig. 9.** Comparison of leaf+trunk full GORT, ACTS, layered Beer's Law and EVI-derived canopy gap probabilities ( $P_{gap}$ ) at a  $5^\circ$  zenith angle bands in a two-layer *Eucalyptus* forest, Tumbarumba flux tower site, New South Wales, Australia.

ments was small, plot size, and revealed importance of sample size and the sensitivity of the model to parameter uncertainty. Four categories of parameters are essential for transmittance simulation: canopy geometry, PAI, end member spectral reflectance and transmittance, and solar zenith angle. Better parameterization increases the accuracy of the simulation, as well as the understanding of the whole scenario.

Canopy geometry can be acquired from allometric equations and field measurements. In modeling studies, tree size and foliage density can be calculated from some empirical formula based on the measurement of DBH and knowledge of plant functional type (Pacala et al., 2001; Albani et al., 2006), but these relationships could be too general to fit the needs of validation, which is more site-specific. For field measurement of canopy geometry, the mean

horizontal and vertical crown radii,  $R$ ,  $b$ , and tree density,  $\lambda$ , are fairly easy to determine. The lower and upper crown centers at  $h_1$  and  $h_2$  can be calculated from the recording of canopy height  $h_0$ , e.g., for a crown center height for a single tree  $h_c = h_0 - b$ , and, with a probability of 95%,  $h_1$  and  $h_2$  fall within the range of mean  $(h_c) \pm 3\text{std}(h_c)$ ; the range can be adjusted according to the real situation.

In contrast, plant area volume density  $P_a$  (plant area per crown volume) is usually derived using this equation, which requires the knowledge of PAI (plant area index):  $P_a = \text{PAI} / ((4/3)\lambda\pi R^2 b)$ . PAI parameterization can be achieved from allometric equations, non-destructive indirect field measurements, and remote sensing retrievals. Allometric equations to derive PAI suffer the same aforementioned problems. Optical measurements of PAI could also

be biased. First, optical measurements still only provide effective PAI measurements e.g., LAI-2000 measurements, or do so in a semi-empirical way (TRAC or fisheye measurements). Ancillary information on structural properties of canopies is required to correct the retrievals for grouping of vegetation elements at shoot and crown levels (Chen et al., 1997). Vegetation clumping and saturation of the optical signal reduce the accuracy of PAI measurements in high PAI stands (broadleaf forests). Second, automated processing of optical PAI measurements does not distinguish between green leaves and dead or stem materials. The removal of such effects can be tedious if it is done with manual processing of images from a fisheye camera or requires specific allometric relations to convert plant area index to leaf area index (Yang et al., 2006). Large uncertainty of PAI might pose a challenge to fully evaluate our model.

Solar zenith angle regulates the path length into the canopy and sunlit/shaded leaf partitioning indirectly through the clumping factor. As it is highly nonlinear, the average of the results spanning large ranges of solar zenith angle can provide only conceptual transmittance profiles, as shown in Figs. 3–5. A weighted average can do a better job. This problem can be eliminated by limiting the time period for the simulation scene. That the clumping factor can vary by solar zenith angle indicates its importance for understory and overstory community dynamics particularly with regard to vegetation at different latitudes.

The clumping factor can be measured using TRAC (Chen and Cihlar, 1995; Chen, 1996), or be derived from the relationship between an angular index (normalized difference between hotspot and darkspot) and the clumping index through a geometrical optical model named '4-Scale' (Lacaze et al., 2002; Chen et al., 2003, 2005; Leblanc et al., 2005). We did not have direct measures of clumping, but the ACTS model (Ni-Meister et al., 2010) adapts a simple formula to calculate the clumping factor, with results demonstrating good agreement with light profile measurements and the importance of this factor for accurate prediction of the light or gap probability profiles.

To our knowledge, this is the first time that data on the canopy vertical profile of light transmittance have been used to evaluate the canopy radiative transfer model designed for land biophysics model or a DGVM. Some prior studies related to canopy radiative transfer used in a land surface model focus more on evaluating and improving model parameterization of surface albedo (Sellers et al., 1996; Zhou et al., 2003; Tian et al., 2004; Wang et al., 2004) using satellite observation. Spatially explicit modeling of canopy radiative transfer was evaluated by Mariscal et al. (2004) at the Wind River Canopy Crane Research Facility (WRCCRF), but such explicit representation is not computationally feasible for use in a DGVM. Chen et al. (2008) derive an analytical clumping factor in a Markov model for a canopy with trees represented as tall boxes at a California blue oak savanna, and they compare results to a the spatially explicit MAESTRA model (Medlyn, 2004) and a Poisson model. Their remarks on the need for representation of more realistic crowns, particularly for conifers, and of shoot clumping, are addressed by the work presented here.

## 5. Conclusion

This study compares to measurements a simple ACTS approach to model the light interaction in heterogeneous plant canopies by integrating a well-described actual vertical foliage profile and a foliage clumping factor.

This model takes into account the vegetation vertical structure heterogeneity by integrating a well-described actual vertical foliage profile. This enhanced multilayer feature allows more precise description of different biological properties of leaves in different layers, such as photosynthetic capacity response to sat-

urated or subdued light gradients with the depth into a canopy (Sellers et al., 1992).

The ACTS model simulations fit ground PAR profile and lidar measurements exceptionally well: in mid- to dense-canopies, the simple ACTS model output demonstrates the importance of clumping (broadleaf deciduous at Morgan-Monroe State Forest and Harvard Forest); in sparse or leafless canopies, and in modeling ground lidar gap probabilities, the trunk effect needs to be accounted for (Morgan-Monroe State Forest, leafless season; Tumberumba, Australia, pine and *Eucalyptus* sites). Meanwhile, as expected, in canopies with little clumping, there is no significant difference from a Beer's law approximation (BOREAS sites). In all cases and for different vegetation types, the model captures the main features of the PAR transmittance of plant canopies, including the sigmoid shape with the vertical height change and hockey stick shape with the solar zenith angle change.

In summary, with excellent accuracy and wide adaptability to various situations demonstrated in this validation work, the ACTS model achieves better or similar performance compared to the full GORT model with respect to field measurements and computational cost. Also, it has advantages relative to the currently widely used two-stream scheme in providing better radiation estimation for photosynthesis by accounting for the impact of both vertical and horizontal vegetation structural heterogeneity on radiative transfer with minimal computational cost.

While this paper focuses on validation results in transmission, our long-term research is to improve the model to describe more realistic canopy radiation absorption and reflection, and to provide a useful scheme for DGVMs. Future papers will provide a description of implementation of the ACTS model in the Ent DGTEM, and evaluation of calculated albedo, photosynthetic fluxes, and the surface energy balance. This will include investigation of the impact of including foliage clumping on simulated photosynthesis and transpiration, the canopy albedo and energy balance, and community dynamics. The foliage clumping factor (Nilson, 1971; Chen and Black, 1992; Stenberg et al., 1994; Stenberg, 1996; Chen, 1996) not only affects the gap fraction for the same LAI, but also can be used to characterize the leaf spatial distribution pattern with a better partitioning of the solar radiation distribution over sunlit and shaded leaves, and between understory and overstory. Thus, without a large addition of computational cost, it can improve the modeling of the carbon cycle over those models that relate carbon absorption simply to intercepted solar radiation (Chen et al., 2003).

## Acknowledgements

The work is supported by NASA under contract NNX06AD06G. We also thank Geoffrey Parker from Smithsonian Environmental Research Center, MD for lending us his giant helium balloon and Shihyan Lee for helping field data collected in Harvard Forest, MA in 2006. The authors are indebted to David L. B. Jupp and Darius. Culvenor from CSIRO for providing the hemispherical ground lidar data collected in Australia and to Steven Wofsky and J. William Munger from Harvard University for providing tree geometry measurements in Harvard Forest. We thank two reviewers for their valuable comments on this paper.

## References

- Albani, M., Medvigy, D., Hurtt, G.C., Moorcroft, P.R., 2006. The contributions of land-use change, CO<sub>2</sub> fertilization, and climate variability to the Eastern US carbon sink. *Global Change Biol.* 12 (12), 2370–2390.
- Barford, C.C., Wofsy, S.C., Goulden, M.L., Munger, J.W., Pyle, E.H., Shawn, P., Urbanski, S.P., Hutyra, L., Saleska, S.R., Fitzjarrald, D., Moore, K., 2001. Factors controlling long- and short-term sequestration of atmospheric CO<sub>2</sub> in a mid-latitude forest. *Science* 294 (5547), 1688–1691, doi:10.1126/science.1062962.

- Chen, J.M., Black, T.A., 1992. Defining leaf area index for non-flat leaves. *Plant Cell Environ.* 15, 421–429.
- Chen, J.M., Cihlar, J., 1995. Plant canopy gap size analysis theory for improving optical measurements of leaf area index. *Appl. Opt.* 34, 6211–6222.
- Chen, J.M., 1996. Optically-based methods for measuring seasonal variation of leaf area index in boreal conifer stands. *Agric. Forest Meteorol.* 80, 135–163.
- Chen, J.M., Rich, P.M., Gower, S.T., Norman, J.M., Plummer, S., 1997. Leaf area index of boreal forests: theory, techniques, and measurements. *J. Geophys. Res.* 102, 29429–29443.
- Chen, J.M., Liu, J., Leblanc, S.G., Lacaze, R., Roujean, J.-L., 2003. A demonstration of the utility of multi-angle remote sensing for estimating carbon absorption by vegetation. *Remote Sens. Environ.* 84, 516–525.
- Chen, J.M., Menges, C.H., Leblanc, S.G., 2005. Global mapping of foliage clumping index using multi-angular satellite data. *Remote Sens. Environ.* 97, 447–457.
- Chen, Q., Baldocchi, D., Gong, P., Dawson, T., 2008. Modeling radiation and photosynthesis of a heterogeneous savanna woodland landscape with a hierarchy of model complexities. *Agric. Forest Meteorol.* 148 (6–7), 1005–1020.
- Ehman, J.L., Schmid, H.P., Grimmond, C.S.B., Randolph, J.C., Hanson, P.J., Wayson, C.A., Cropley, F.D., 2002. An initial intercomparison of micrometeorological and ecological inventory estimates of carbon exchange in a mid-latitude deciduous forest. *Global Change Biol.* 8, 575–589.
- Jupp, D.L.B., Lovell, J., 2004. Product Background and Description for Airborne (VSIS) and Ground-Based (Echidna®) Canopy Lidar Systems. CSIRO Earth Observation Centre, Canberra, ACT, Australia.
- Jupp, D.L.B., Culvenor, D.S., Lovell, J., Newnham, G., 2005. Evaluation and Validation of Canopy Laser Radar (LIDAR) Systems for Native and Plantation Forest Inventory. CSIRO Earth Observation Centre and CSIRO Forestry and Forest Products Division, Canberra, ACT, Australia, 150 pp.
- Jupp, D.L.B., Culvenor, D.S., Lovell, J., Newnham, G., Strahler, A.H., Woodcock, C.E., 2009. Estimating forest LAI profiles and structural parameters using a ground based laser called “Echidna®”. *Tree Physiol.* 29 (2), 171–181, doi:10.1093/treephys/tpn022.
- Lacaze, R., Chen, J.M., Roujean, J.L., Leblanc, S.G., 2002. Retrieval of vegetation clumping index using hotspot signatures measured by the POLDER instrument. *Remote Sens. Environ.* 79, 84–95.
- Law, B.E., Van Tuyl, S., Cescatti, A., Baldocchi, D.D., 2001. Estimation of leaf area index in open-canopy ponderosa pine forests at different successional stages and management regimes in Oregon. *Agric. Forest Meteorol.* 108, 1–14.
- Leblanc, S.G., Chen, J.M., White, H.P., Latifovic, R., 2005. Canadawide foliage clumping index mapping from multi-angular POLDER measurements. *Can. J. Remote Sens.* 31 (5), 364–376.
- Leuning, R., Cleugh, H.A., Zegelin, S.J., Hughes, D., 2005. Carbon and water fluxes over a temperate Eucalyptus forest and a tropical wet/dry savanna in Australia: measurements and comparison with MODIS remote sensing estimates. *Agric. Forest Meteorol.* 129, 151–173.
- Li, X.W., Strahler, A.H., 1988. Modeling the gap probability of a discontinuous vegetation canopy. *IEEE Trans. Geosci. Remote Sens.* 26 (2), 161–170.
- Mariscal, M.J., Martens, S.N., Ustin, S.L., Chen, J., Weiss, S.B., Roberts, D.A., 2004. Light-transmission profiles in an old-growth forest canopy: simulations of photosynthetically active radiation by using spatially explicit radiative transfer models. *Ecosystems* 7 (5), 454–467.
- Medlyn, B.E., 2004. A MAESTRO retrospective. In: Mencuccini, M., Grace, J.C., Moncrieff, J., McNaughton, K. (Eds.), *Forests at the Land–Atmosphere Interface*. CAB International, pp. 105–121.
- Ni, W.G., Li, X.W., Woodcock, C.E., Roujean, J.L., Davis, R.E., 1997. Transmission of solar radiation in boreal conifer forests: measurements and models. *J. Geophys. Res.* 102 (D24), 29555–29566.
- Ni-Meister, W., Jupp, D.L.B., Dubayah, R., 2001. Modeling lidar waveforms in heterogeneous and discrete canopies. *IEEE Trans. Geosci. Remote Sens.* 39 (9), 1943–1958.
- Ni-Meister, W., Strahler, A.H., Woodcock, C.E., Schaaf, C., Jupp, D.L.B., Yao, T., Zhao, F., Yang, X., 2008. Modeling the hemispherical scanning, below-canopy lidar and vegetation structure characteristics with a geometric optical and radiative transfer model. *Can. J. Remote Sens.* 34 (S2), S385–S397.
- Ni-Meister, W., Yang, W., Kiang, N.Y., 2010. A clumped-foliage canopy radiative transfer model for a global dynamic terrestrial ecosystem model I: Theory. *Agric. Forest Meteorol.*, doi:10.1016/j.agrformet.2010.02.009.
- Ni-Meister, W., Lee, S., Strahler, A.H., Woodcock, C.E., Schaaf, C., Sun, G., Ranson, K.J., Blair, J.B., in press. Assessing a general relationship between plot level above ground biomass, vegetation structure and vegetation Lidar. *J. Geophys. Res.*
- Nilson, T., 1971. A theoretical analysis of the frequency of gaps in plant stands. *Agric. Forest Meteorol.* 8, 25–38.
- Olyphant, A.J., Grimmond, C.S.B., Zutter, H.N., Schmid, H.P., Su, H.B., Scott, S.L., Offerle, B., Randolph, J.C., Ehman, J., 2004. Observations of energy balance components in a temperate deciduous forest. *Agric. Forest Meteorol.* 126, 185–201.
- Olyphant, A.J., Rose, W., Schmid, H.P., Grimmond, S., 2006. Observations of canopy light penetration and net ecosystem exchange of CO<sub>2</sub> under different sky conditions in a mid-western mixed deciduous forest. In: 27th Conf. Agric. Forest Meteorol. 43.
- Pacala, S.W., Hurr, G.C., Baker, D., Peylin, P., Houghton, R.A., Birdsey, R.A., Heath, L., Sundquist, E.T., Stallard, R.F., Ciais, P., Moorcroft, P., Caspersen, J.P., Shevliakova, E., Moore, B., Kohlmaier, G., Holland, E., Gloor, M., Harmon, M.E., Fan, S.-M., Sarmiento, J.L., Goodale, C.L., Schimel, D., Field, C.B., 2001. Consistent land-and atmosphere-based US carbon sink estimates. *Science* 292, 2316–2320, doi:10.1126/science.1057320.
- Schmid, H.P., Grimmond, C.S.B., Cropley, F., Offerle, B., Su, H.-B., 2000. Measurements of CO<sub>2</sub> and energy fluxes over a mixed hardwood forest in the midwestern US. *Agric. Forest Meteorol.* 103, 357–374.
- Sellers, P.J., Berry, J.A., Collatz, G.J., Field, C.B., Hall, F.G., 1992. Canopy reflectance, photosynthesis, and transpiration. III. A reanalysis using improved leaf models and a new canopy integration scheme. *Remote Sens. Environ.* 42, 187–216.
- Sellers, P.J., Hall, F.G., Kelly, R.D., Black, A., Baldocchi, D., Berry, J., Ryan, M., Ranson, K.J., Crill, P.M., Lettenmaier, D.P., Margolis, H., Cihlar, J., Newcomer, J., Fitzjarrald, D., Jarvis, P.G., Gower, S.T., Halliwell, D., Williams, D., Goodison, B., Wickland, D.E., Guertin, F.E., 1997. BOREAS in 1997: experiment overview, scientific results and future directions. *J. Geophys. Res.* 102 (D24), 28731–28770.
- Sellers, P.J., Los, S.O., Tucker, C.J., Justice, C.O., Dazlich, D.A., Collatz, G.J., Randall, D.A., 1996. A revised land surface parameterization (SiB2) for atmospheric GCMs. Part II. The generation of global fields of terrestrial biophysical parameters from satellite data. *J. Climate* 9, 706–737.
- Stenberg, P., Kuuluvainen, T., Kellomaki, S., Grace, J.D., Jokela, E.J., Gholz, H.L., 1994. Crown structure, light interception and productivity of pine trees and stands. *Ecol. Bull.* 43, 20–34.
- Stenberg, P., 1996. Correcting LAI2000 estimates for the clumping of needles in shoots of conifers. *Agric. Forest Meteorol.* 79, 1–8.
- Strahler, A.H., Jupp, D.L.B., Woodcock, C.E., Schaaf, C.B., Yao, T., Zhao, F., Yang, X., Lovell, J., Culvenor, D., Newnham, G., Ni-Meister, W., Boykin-Morris, W., 2008. Retrieval of forest structural parameters using a ground-based lidar instrument (Echidna®). *Can. J. Remote Sens.* 34 (Suppl. 2), S426–S440.
- Tian, Y., Dickinson, R.E., Zhou, L., Myneni, R.B., Friedl, M., Schaaf, C.B., Carroll, M., Gao, F., 2004. Land boundary conditions from MODIS data and consequences for the albedo of a climate model. *Geophys. Res. Lett.* 31, L05504, doi:10.1029/2003GL019104.
- Wang, Z., Zeng, X., Barlage, M., Dickinson, R.E., Gao, F., Schaaf, C.B., 2004. Using MODIS BRDF and albedo data to evaluate global model land surface albedo. *J. Hydrometeorol.* 5, 3–14.
- Wofsy, S.C., Goulden, M.L., Munger, J.W., Fan, S.M., Bakwin, P.S., Daube, B.C., Bassow, S.L., Bazzaz, F.A., 1993. Net exchange of CO<sub>2</sub> in a mid-latitude forest. *Science* 260 (5112), 1314–1317, doi:10.1126/science.260.5112.1314.
- Yang, W., Tan, B., Huang, D., Rautiainen, M., Shabanov, N.V., Wang, Y., Privette, J.L., Huemmrich, K.F., Fensholt, R., Sandholt, I., Weiss, M., Nemani, R.R., Knyazikhin, Y., Myneni, R.B., 2006. MODIS leaf area index products: from validation to algorithm improvement. *IEEE Trans. Geosci. Remote Sens.* 44 (7), 1885–1898.
- Zhou, L., Dickinson, R.E., Tian, Y., Zeng, X., Dai, Y., Yang, Z.-L., Schaaf, C.B., Gao, F., Jin, Y., Strahler, A., Myneni, R.B., Yu, H., Wu, W., Shaikh, M., 2003. Comparison of seasonal and spatial variations of albedos from moderate-resolution imaging spectroradiometer (MODIS) and common land model. *J. Geophys. Res.* 108 (D15), 4488, doi:10.1029/2002JD003326.